Computational insights about the dynamic behavior for the inclusion process of deprotonated and neutral aspirin in beta-cyclodextrin

Belgacem Bezzina, Rayenne Djémil, Djameleddine Khatmi, Stéphane Humbel, Yannick Carissan

Computational insights about the dynamic behavior for the inclusion process of deprotonated and neutral aspirin in β–cyclodextrin

Belgacem Bezzina,[a,b] Rayenne Djémil,[a] Djameleddine Khatmi,[a, c,*] Stéphane Humbel,[c]

Yannick Carissan[c]

[a] - Laboratory of Computational Chemistry and Nanostructures, Department of Material Sciences, Faculty of Mathematical, Informatics, and Material Sciences, University of 08 May 1945 Guelma, Algeria

[b-] Research Center in Industrial Technology (CRTI), P.O.BOX 64, Chéraga 16014, Algiers, Algeria

[c-] Aix Marseille Univ, CNRS, Centrale Marseille, iSm2, Marseille, France

*correponding author: khatmi.djameleddine@gmail.com

KEYWORDS: Aspirin. cyclodextrin. inclusion complexes. molecular dynamics. quantum mechanics. AIM. NBO.

ABSTRACT: Quantum mechanics and molecular dynamics were used to study the inclusion of neutral and deprotonated aspirin into the β–cyclodextrin (β–CD) cavity. The molecular dynamic simulation allows following the time dependent behavior of the formation of the inclusion complex. For both complexes, we find a reasonable and a realistic pattern of the complexation. The calculations show a single pathway consisting of an irreversible process leading to the complexation of aspirin. Whereas, for deprotonated aspirin it has been observed a reversible complexation, in which one way leads to the binding form, and the reverse way to the unbinding form. Throughout the simulation, the penetration of aspirin (ASA) or deprotonated aspirin (ASA–) inside the cavity occurs only with a phenyl ring entering first through the wider or narrower rim. The Molecular Dynamics (MD) study results in a favorable inclusion process for aspirin and an unfavorable one for the deprotonated aspirin. A few remarkable conformations of the neutral complex were examined in particular detail. The lowest energy minimum structures of the complexes are obtained with B3LYP/cc-pvdz calculations. The neutral aspirin complex, wherein the guest is deeply embedded inside the cavity, is found more favorable than the deprotonated one, which is partially included. These geometries are well characterized by UV and IR calculation spectra, and confirm the consistency of both the MD results and the experimental observations. The intermolecular interactions between the aspirin and β–CD are modeled by the NBO and AIM methods. Finally, it turned out, that the most important driving forces of the complexation are, the hydrogen bonds, and the hydrophobic/hydrophilic interactions.

1- INTRODUCTION

An inclusion complex – a combination of two or more species - is based on a non-covalent interactions between the host and guest molecules and their stability depends on the size and complementary forms of host and guest molecules. Additionnaly, the external medium and environmental conditions can also play a role [1, 4].

β–cyclodextrin (β–CD) is a cyclic oligosaccharide derived by enzymatic hydrolysis of common starch. Due to its peculiar chemical structure, constituted of an external hydrophilic surface and a hydrophobic cavity, β–CD can form inclusion complexes with a variety of organic molecules, thereby improving some of their properties, such as solubility, stability and bio-availability [5-7].

The main forces involved in the complexation process are electrostatics, van der Waals, hydrophobic interactions, hydrogen bonding and charge transfer interactions [8-10]. The complexation process in solution comprises several steps, which we briefly summarize here: at first, as the guest molecule approaches the β-CD cavity, it is released from the hydration layer which surrounded it, and conjointly the water molecules which are inside the cavity are released outside. Then, the guest molecule penetrates inside the β-CD cavity giving a chemical complex stabilized only by non-covalent interactions [8].

If the guest molecule finds a great stability inside the cavity, it will remain there for a long time, and the process can be considered as an irreversible binding process. Otherwise, without large stabilizing interactions with the host molecule inside the cavity, it will be released and water molecules would return in the cavity. However, the guest molecule can return inside the cavity so the process is considered as a reversible binding process which can occur repeatedly [11].

Several factors may influence the inclusion complex formation, such as the type of CD, cavity size, pH and ionization state, temperature and method of preparation [12]. For instance, when the guest molecule is negatively charged it reduces its complexation ability compared to the neutral form. This is due to the fact that the negative charge reduces the hydrophobicity of the guest molecule and impedes its penetration inside the hydrophobic cavity [13].

The molecular encapsulation process has constituted a major area of expertise and investigation within the framework of supramolecular chemistry. It became the subject of intense

experimental and theoretical studies because the detailed knowledge of the dynamics of complexation constitutes the basis of its use as a drug carrier [12-19].

Acetylsalicylic acid (ASA), also known by the trade name aspirin, is one of the most known, used and popular drugs. It belongs to a group of medication called non-steroidal anti-inflammatory drug (NSAIDs); it is often used to treat pain [18], fever [19], inflammation [20], to help prevent heart attacks [21], blood clot formation [22], and in a certain type of cancer, as colorectal or pancreatic cancer [23, 24].

The spontaneous hydrolysis of aspirin vary markedly with pH. At pH below 2.5 aspirin is in its neutral form, whereas, at higher pH it becomes increasingly deprotonated. Its rate of absorption in the stomach, which has a pH of 1.5 to 3.5 depends on its form. Thus, the majority of the biological activities, attributed to the neutral form is due to its lipophilic nature, which facilitates its absorption through the stomach wall, and its passing into the bloodstream [25, 26].

In many cases their use at higher doses can generate bad side effects, notably gastric irritation, gastrointestinal ulcers, hematemesis, tinnitus and stomach bleeding [27, 28]. These inconveniences are due, in particular, to its low solubility in water estimated to 1 g/300 ml [29], caused by its rapid decomposition in two acids, salicylic and acetic [30].

Several methods are used to overcome these inconveniences such as its use as a pro drug or microencapsulation. The microencapsulation system, also named inclusion complex, is constituted of two molecules forming a single entity in which the molecule called "guest" is trapped in the cavity of another one, called "host"; and the system is stabilized only by non-covalent interactions [31, 32].

The application of the microencapsulation technique, allows improving the apparent solubility of poorly soluble molecules, protecting the fragile ones from unfavorable conditions and enhancing its therapeutic properties, such as its use as a drug delivery system (DDS) [33–41].

Many authors have studied the complexation process of aspirin with β–cyclodextrin using various techniques such as X-ray (RX) [42, 43], spectroscopic methods [44–48], ultrasonic relaxation [49], and isothermal calorimetric titration [27]. These studies led to the following conclusions: (i) the inclusion is deep with neutral aspirin (ASA) and partial with the deprotonated form (ASA^-); (ii) the phenyl moiety of neutral aspirin is localized inside the cavity, whereas, with the deprotonated form it is largely outside; (iii) hydrophobic interactions and hydrogen bonds play the major role in the complexation.

However, there are still outstanding issues that deserves further studies, such as the evolution of complexation process and the effect of the inclusion on ultraviolet (UV) and infrared (IR) spectra.

Computational chemistry methods can give appropriate answers because they have already had a great success in solving several problems related to the geometry, the physical chemistry, and the driving forces of the complexation [50–54].

The number of published papers in the past decade on this topic has widely increased, showing the evidence of a passion, attesting the mastery and the growing knowledge on the subject [55-57]. Furthermore, while the pH is of primary importance for its biological effect, to the best of our knowledge, there are no reports in the literature on the evolution of the complexation of β–CD with neutral vs deprotonated aspirin. This also motivated the present study.

For this purpose, we describe, in this article, a computational study on the complexation process between neutral/deprotonated aspirin and β–CD using molecular dynamics and quantum mechanics. Then, the spectral calculations with B3LYP/cc-pvtz were used to provide a clear picture and to gain significant knowledge on these complexes. Finally, we shall focus our attention on the hydrogen bonds, one of the main driving forces of the complexation by using both natural bond orbital (NBO) and atoms in molecules (AIM) methods.

2- METHODS

The initial geometry of the system is prepared using the graphical interface of the ChemBioOffice software. The initial structure of β–CD was built with the help of ChemBioOffice (version 10, Cambridge software) [58], and the geometry of aspirin was extracted from a PubChem Compound Database [59] (Figure 1). Two possible orientations were considered. When complexation occurs by the wider side is called “orientation A” and when it occurs by the narrower side is called “orientation B”.

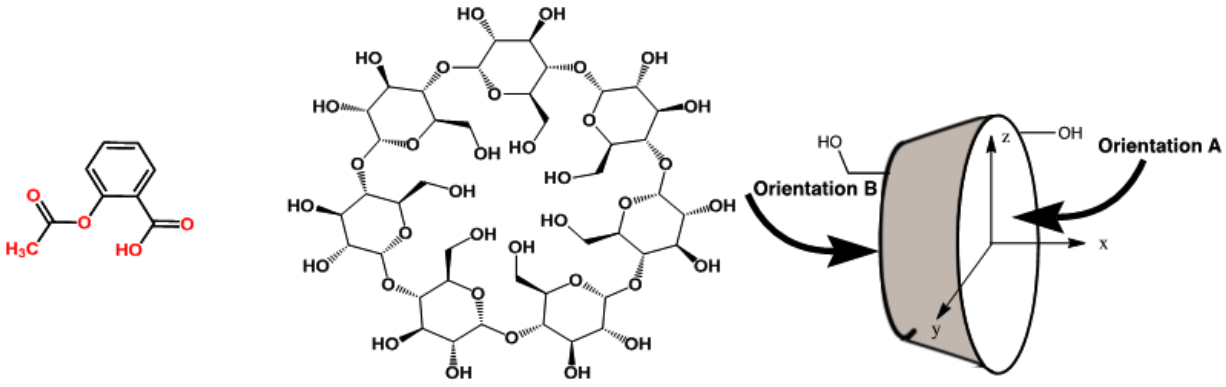

Figure 1. Aspirin and β–CD molecular structures

Two methodological approaches were used to describe the inclusion process, automatic for molecular dynamics and manual for quantum mechanics.

2.1 Molecular dynamics

First, β–CD is fixed in the center of XYZ coordinate system. Then, neutral/deprotonated aspirin is placed on the X-coordinate axes at a distance equal to 14 Å from the center of β–CD (Figure 1, 2).

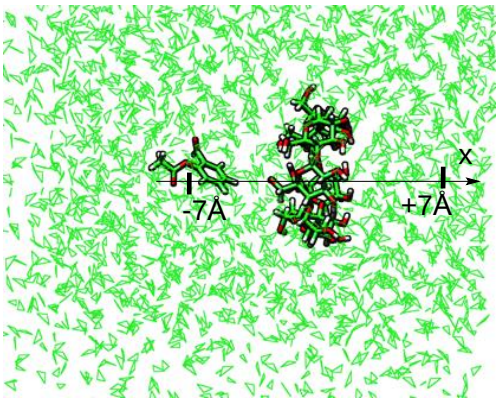

Figure 2 The initial geometry of the aspirin and β–CD molecules in the water box at the beginning of the simulation.

The force field parameters for both molecules were generated using the automated topology builder (ATB) [60] in the framework of GROMOS96 54A7 force field [61] [see supplementary materials].

All simulations were carried out using the GROMACS package version 5.2.1 into an identical box containing 2638 water molecules represented by a simple point charge (SPC) model [62,

63]. The simulations were performed in the isobaric-isothermal ensemble (NPT) with a constant pressure of 1 bar and a temperature of 298 K controlled by the Berendsen thermostat. The electrostatic interactions were treated by the particle mesh Ewald (PME) method with a cutoff distance of 1.2 nm; and the van der Waals interactions were modeled using a cutoff of 1.4 nm. The whole system was relaxed using the steepest descent algorithm. The position of the guest molecule is obviously altered after the equilibration steps. The classical Newton's equations of motion were integrated using the Leap-Frog algorithm and the Berendsen weak-coupling method. All simulations were carried out for 1000 ns, which is long enough for the system to reach equilibrium. The trajectory coordinates were recorded every 500 steps with a time step of 1 fs.

2.2 Quantum mechanical calculations

All quantum chemistry calculations were carried out using the Gaussian 09 package [64]. To define the aspirin:β–CD inclusion complex, the glycosidic oxygen atoms of β–CD were placed onto the YZ plane, the center of β–CD being defined as the origin of the coordinate system. The relative position between β–CD and Aspirin is measured by the X coordinate of the center of the aromatic ring of Aspirin. Aspirin was initially located on an X-coordinate equal to 7 Å and was moved into the β–CD cavity along the X axis to – 7 Å with a 1 Å step (figure 2). The generated structures at each step were optimized with the PM3 semi empirical method, allowing them to change from the initial conformations keeping the displacement of the center of the aromatic ring and the β–CD.

Then, the complexation energy of all structures was calculated by using the following expression:

$$\Delta E_{\text{complexation}} = E_{\text{complex}} - (E_{\text{free aspirin}} + E_{\text{free β–cyclodextrin}}) \qquad Eq.1$$

E_{complex} is the heat of the formation of the complex, $E_{\text{free aspirin}}$ and $E_{\text{free β–cyclodextrin}}$ are the energies of aspirin and β–cyclodextrin molecules in their free state. The more negative is the complexation energy, the more thermodynamically favorable is the inclusion complex.

The two lowest energy minimum structures of the neutral ASA**:**β–CD and the deprotonated ASA^{-}**:**β–CD complexes were optimized with the B3LYP/cc-pvdz method [65–69].

2.3 NBO and AIM analysis

The stabilization energy $E^{(2)}$ related to the delocalization trend of electrons from a donor to acceptor orbitals, is calculated with the NBO method [70]. A large stabilization energy $E^{(2)}$ from the LP(Y) lone pair of the proton acceptor to the σ* (X-H) anti-bonding orbital of proton donor is generally indicative of an X-H···Y hydrogen bond [71-74].

Finally, by means of AIM2000 software [75], a topological analysis of electron density with Bader's theory of atoms in molecules (QTAIM) [76-77] is applied on the free neutral/deprotonated aspirin (ASA/ASA^-) and their most favorable complex obtained with B3LYP/cc-pvdz method. The wave functions required for this analysis were generated after performing a single point calculation at the same level of theory.

2.4 IR and UV spectra

The infrared spectra of the neutral/deprotonated (ASA / ASA^-) free aspirin, free β–CD and their inclusion complex were calculated at the B3LYP/cc-pvdz level using CPCM model with acetonitrile as a solvent.

Time-dependent density functional theory (TD-DFT) is used to characterize the vertical excitation (reference) of all compounds. Thus, from the fundamental geometry of a complex, we modelled its absorption spectrum by the analysis of the linear response of the ground state density to a time-dependent perturbation (TD-DFT calculations). We simulate the photoexcitation and we analyze the set of electronic transitions that results. This calculation gives access to the energy necessary to drive each transition and to the associated oscillator force when it corresponds to an allowed transition (here we refer to the spectroscopic selection rules). The intensity of these transitions is thus obtained, and it is then possible to plot the absorption spectra.

Finally, the UV-vis spectra of free neutral/deprotonated (ASA/ASA^-) free β–CD and their inclusion complex were calculated at the B3LYP/cc-pvdz level using CPCM model with ethanol as a solvent.

3- Results and discussions

3.1 Molecular dynamics

Three independent molecular dynamics simulations of 1000 ns were performed to describe the inclusion process of neutral/deprotonated (ASA/ASA⁻) aspirin with β–CD at the molecular level. The simulations with the neutral aspirin are reported in figure 3, with the labels S1, S2, S3 and those with the deprotonated aspirin are in figure 6 (S'1, S'2, S'3).

3.1.1. The inclusion process of aspirin with β–CD

Throughout the simulation, the inclusion process is described through the analysis of the variation of the distances between the two centroïds of mass of aspirin and β–CD (Figure 3). In all three simulations it was observed that the penetrations and exits of aspirin in and out of the cavity can occur. As it can be seen in Figure 3, three interesting facts are emerging from the three simulations: (i) a rapid penetration of aspirin, which can last only a few ns, followed by a long stay inside the cavity; it remains there deeply embedded until the end of the simulation; except of the S'2 simulation where around 400 ps aspirin briefly leaves the cavity and returns rapidly inside. (ii) also, there are some regions where there are more fluctuations, indicating that aspirin moves in these regions freely inside the cavity, exceeding sometimes the limits of the cavity with respect to the steps. (iii) changes of the aspirin orientation inside the β–CD cavity occur during the simulations, from A to B or the reverse, these changes of orientation are made via a few unbound forms (Figure 4).

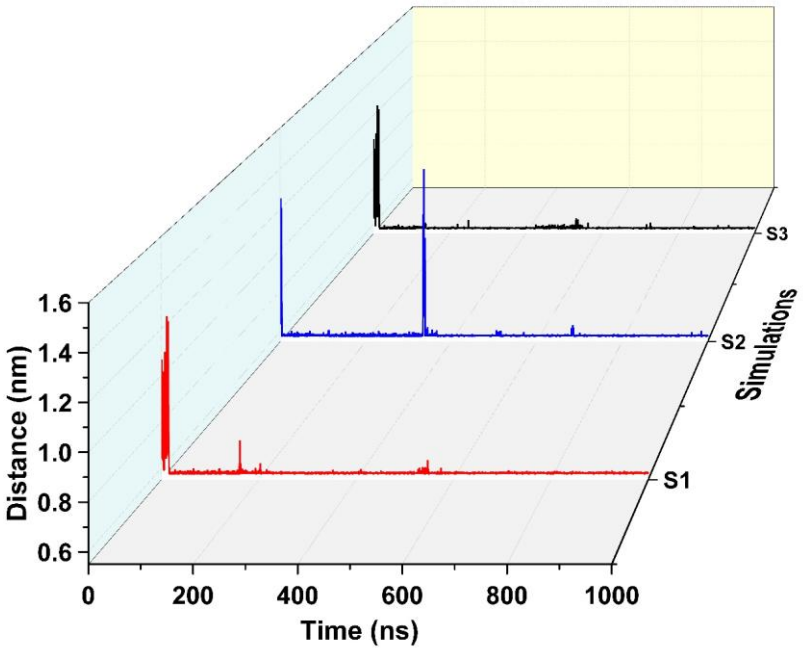

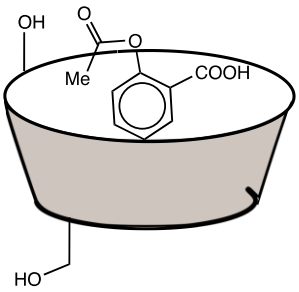

Figure 3. The plot of the variation of the distance between the two centroïds of mass of aspirin and β–CD during the three simulations.

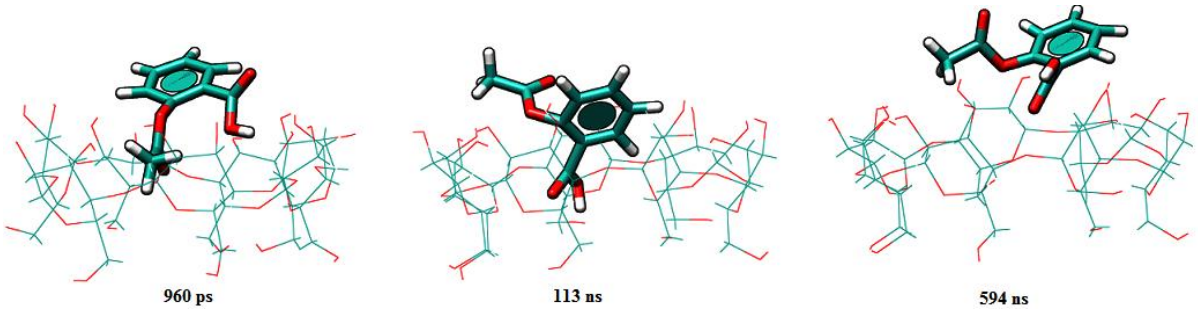

Figure 4. Snapshots showing the unbound states at 960, 113 and 594 ns, of the neutral complex extracted from S'1 simulation.

From these simulations, four key points are highlighted: (i) mostly the complexation process is irreversible (ie, once aspirin penetrates into the cavity, it is no longer available in the medium); (ii) aspirin can penetrated by the two entrances; (iii) the inclusion complex is favorable in aqueous medium because aspirin spent much more time inside the cavity, 982 (S1), 988 (S2) and 997 (S3) ns than the outside; (iv) the orientation A is more favorable than the B one, because the lifetime of the orientation A is larger than that of orientation B: the orientation A lasts 814 (S1), 705 (S2) and 846 (S3) ns while B lasts 167 (S1), 283 (S2) and 150 (S3) ns. In Figure 5 are displayed the averaged geometries of the ASA:β–CD complex in the A and B orientation. In the A orientation aspirin is deeply embedded inside the cavity, whereas in the orientation B only the phenyl ring is included and the functional groups stay in secondary periphery establishing hydrogen bonds with β–CD.

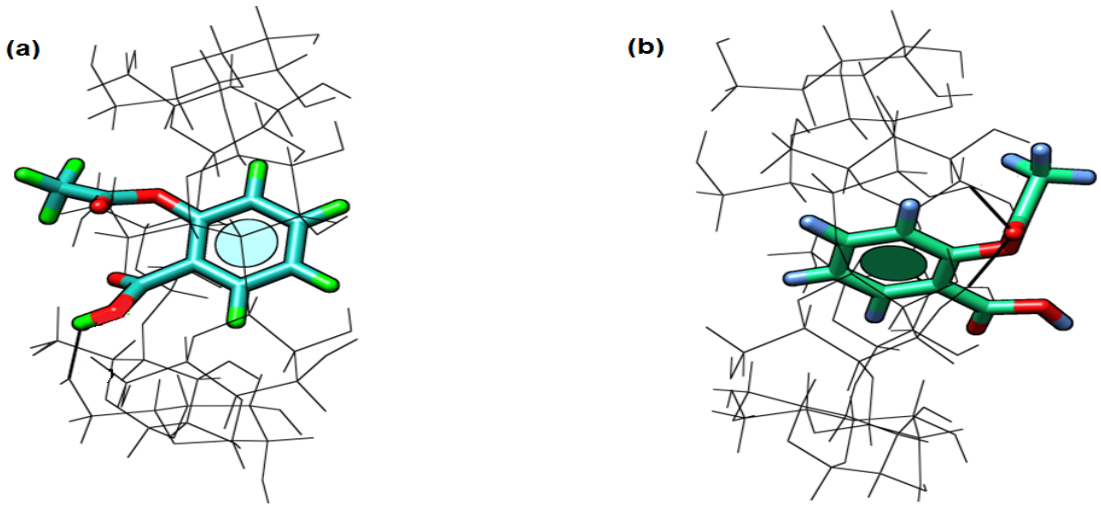

Figure 5. Averages geometries of the ASA:β–CD complex, (a) orientation A (b) orientation B

3.1.2 The inclusion process of deprotonated aspirin with β–CD

The simulations are labelled S'1, S'2, S'3, and they are shown on Figure 6. Throughout all three simulations it was observed, that the phenyl group penetrates first through the wider or narrower side with equal proportions. The penetration of deprotonated aspirin is incomplete : only the phenyl group enters the β–CD cavity, whereas the acetyl and carboxylate groups remain outside.

As can be seen from Figure 6, the variation of the distance between the center of mass of deprotonated aspirin and β–cyclodextrin is very similar from one simulation to another: S'1 ressembles S'2 and S'3 is alike.

In each simulation, it was observed multiple entrances and exits of deprotonated aspirin of the cyclodextrin cavity. At each time, the guest molecule remains only a small moment inside the cavity with the exception of the periods [300-450] for S'1, [200-310] for S'2 and [700-790] ns for S'3 where it passes more than 100 ns inside the cavity.

Overall, these three simulations are not in favor of an inclusion process because the guest molecule spent more time outside the cyclodextrin cavity, and moves freely in the aqueous medium. For the S'1, S'2 and S'3 simulations, this occurs 63, 52 and 67% of the time of simulation, respectively. Moreover, even when within the cavity the guest molecule, is constantly moving along the axis of the cavity and adopts a fairly large number of conformations, indicating its instability inside.

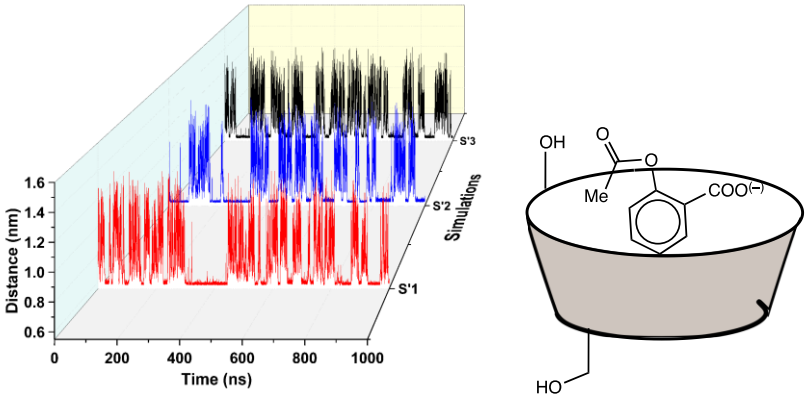

Figure 6. The variation of the distance between the mass centers of deprotonated aspirin and β-CD during all the three simulations.

From these simulations, three key points are highlighted: (i) the complexation process is reversible (ie. the guest molecule enter and exit the cavity several times) (ii) deprotonated aspirin penetrates inside the cavity through both the wider or the narrower rim; (iii) the inclusion complex is unfavorable in aqueous medium because deprotonated aspirin spends more time outside the cavity.

3.2. Quantum mechanics

3.2.1 Complexation energies and the structures of the inclusion complexes

Negative values of the complexation energies are synonymous of a favorable process because the more negative is the complexation energy, the more thermodynamically favorable is the inclusion complex. Thus, the complexation energy of the lowest energy minimum structure is found equal to -3.0 to –5.7 kcal.mol^{-1} for the neutral and deprotonated complexes, respectively.

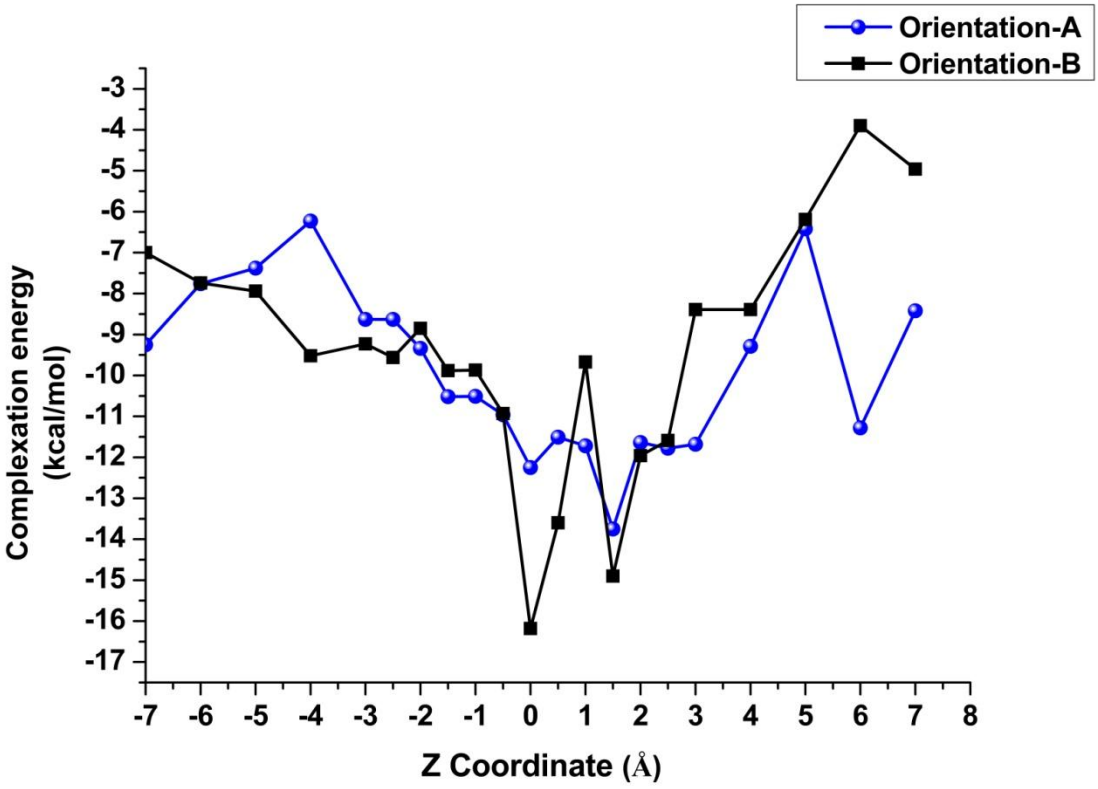

Figure 7. Complexation energy of the neutral ASA:β–CD complex along the z axis.

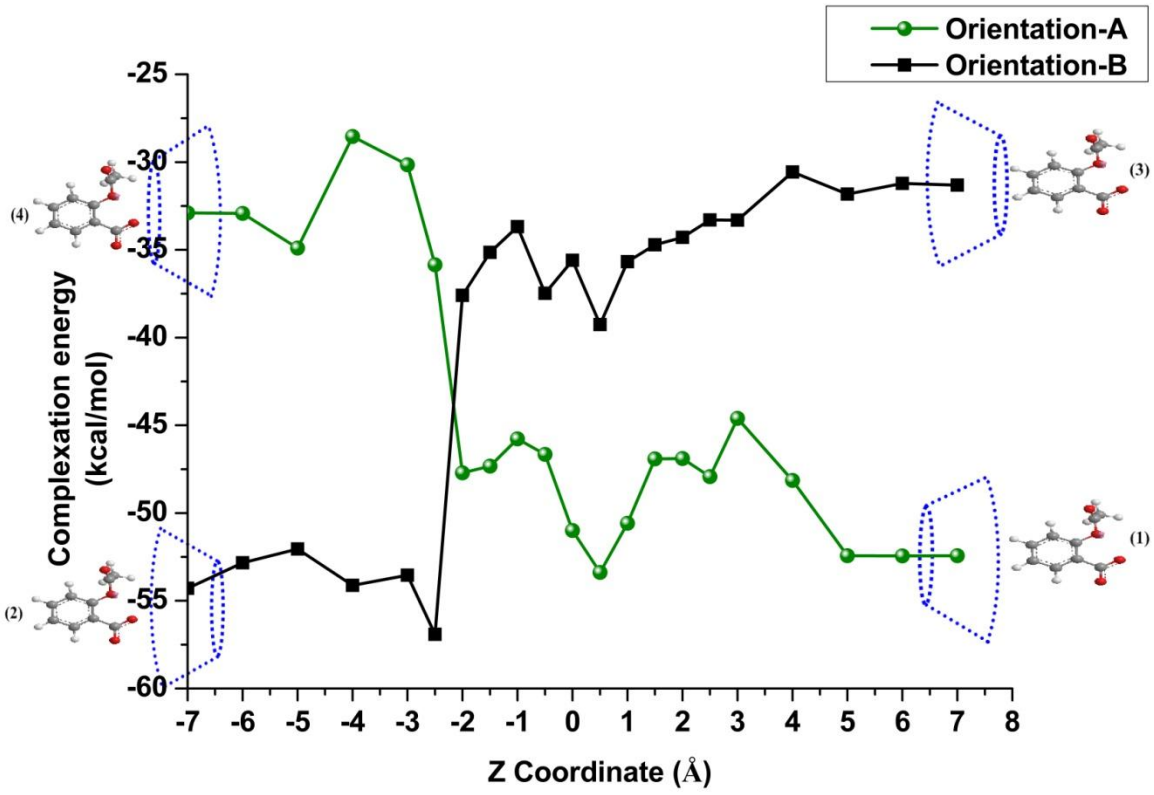

Figure 8. Complexation energy of ASA$^-$:β–CD complex along the z axis.

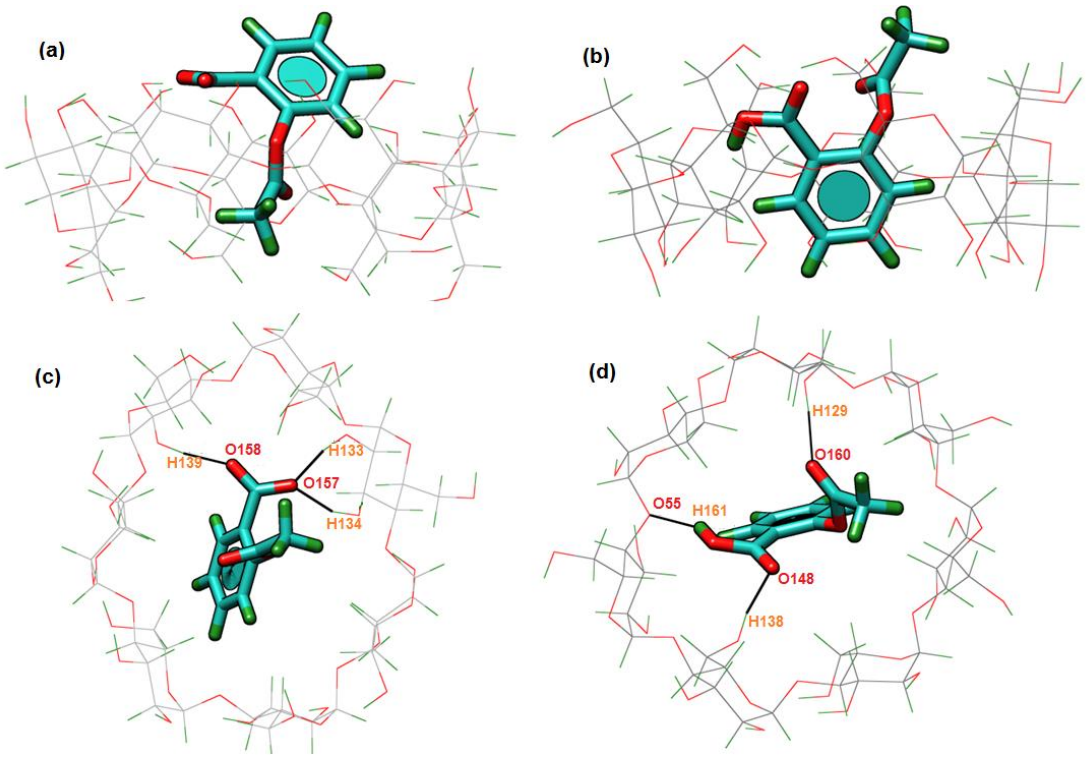

Figure 9 Structures of the B3LYP/cc-pvdz energy minimum obtained for the inclusion complexes. (a),(c) deprotonated form (b), (d) neutral form.

In Figure 9 are displayed the geometries of the two inclusion complexes. The lowest energy minimum of the ASA: β–CD was localized at 0 Å and that of ASA^-:β–CD at -2.5 Å (Figure 7 and 8). It shows clearly that the phenyl group is deeply embedded inside the cavity for the neutral complex, whereas in the deprotonated form it remains outside. The acetyl and carboxylic, of the neutral complex, remain on the narrow rim, where they establish hydrogen bonds with the primary hydroxyls of the β–CD. However, in the deprotonated complex, the acetyl group is located inside the cavity, leaving the carboxylate group on the wide rim establishing three hydrogen bonds with the secondary hydroxyls of the β–CD.

This is in agreement with the experimental results which stipulate that deprotonated ASA- does not form complex with β–CD and neutral ASA form an inclusion complex with establishing several hydrogen bonds with β–CD.

In the following, we will focus only on the lowest energy minimum structures displayed in Figure 9.

3.2.2 Hydrogen bonding and population analysis

The strength of hydrogen bonds and their geometrical parameters (distance and angle) are closely correlated.[ref] The angle between the atoms involved is linear (> 175°), and the shorter the distance (< 2 Å) the stronger the H-bond. Based on several monographs, the hydrogen bonds were classified according to the values of their dissociation energies. Thus, are considered as weak hydrogen bonds those with an energy of 1 to 4 kcal mol^{-1}, moderate for 4 to 15 kcal mol^{-1}, and strong for 15 to 40 kcal mol^{-1} [78-81]. Herein, the strength of the hydrogen bonds cannot be evaluates as a dissociation energy because the dissociation corresponds to several different interactions. Hence we used the $E^{(2)}$ stabilization energy obtained by perturbation within the NBO method. These values as well as the geometrical parameters of these hydrogen bonds of both complexes are given in Table 1.

Table 1. The stabilization energy $E^{(2)}$ obtained with B3LYP/cc-pvdz of the main hydrogen bond interactions and their geometrical parameters of both complexes. The d distance is measured between H and Y atoms in the (X-H···Y) bond, and the angle between X, H and Y atoms implies in the hydrogen bond.

Complex form		**d (Å)**	**Angle (°)**	**$E^{(2)}$ (kcal/mol)**
Neutral				
Aspirin acceptor and β–CD proton donor				
Lp O160	σ*(H129-O47)	1.90	166	5.99
Lp O148	σ*(H138-O62)	1.95	166	4.11
β–CD acceptor and aspirin proton donor				
Lp O55	σ*(H161-O150)	1.97	146	4.65
Deprotonated				
Aspirin acceptor and β–CD proton donor				
Lp O157	σ*(H133-O53)	1.81	167	15.23
Lp O157	σ*(H134-O54)	1.74	152	14.56
Lp O158	σ*(H139-O63)	1.70	171	11.10

Based on, $E^{(2)}$ values and the geometrical parameters, the H-bonds of the neutral complex are significantly weaker, than those of the deprotonated complex.

An inspection of the geometry of the neutral complex (Table 1 and Figure 9) shows that there are two hydrogen bonds where β–CD plays a proton donor role, and it plays an acceptor role in a third one. The first H-bond occurs between O160 of the acetyl group and H129 of the H129-O47 bond of β–CD, and the second between O148 of the carboxylic group and H138 of the H138-O62 of β–CD. The third one occurs between carboxylic hydrogen atom (H161) of the H161-O150 bond of aspirin and a glycosidic oxygen atom (O55) of β–CD.

In the hydrogen bonds of the deprotonated complex, β–CD plays the role of a proton donor, and aspirin of an acceptor. The first H-bond occurs between O158 of the carboxylate group and H139 of the H139-O63 bond of β–CD. However, the oxygen atom O157 of the carboxylate group is positioned so that it participates in two H-bonds; the first one with H133 of the H133-O53 bond, and the second with H134 of the H134-O54 bond.

3.2.3 Hydrogen bonding and AIM analysis

The Bader AIM method provides a physical picture of the interaction between proton donor and acceptor in hydrogen bonding; it is achieved by exploring the topological parameters of the electron density ρ_b. Its Laplacian $\nabla^2\rho_b$ defines different types of critical points.

Several criteria relative to the values of the electron density and its Laplacian reported in the literature were used to classify and characterize hydrogen bonds at bond critical points (BCPs). Thus, it was mentioned that a hydrogen bonding is detected in the range of 0.002-0.04 and 0.024 -0.139 for ρ_b and $\nabla^2\rho_b$ respectively. Larger values of electron density and of its Laplacian give stronger hydrogen bonds [82, 83].

Table 2. Topological analysis obtained with B3LYP/cc-pvdz of the electron density ρ_b and Laplacian $\nabla^2\rho_b$ for the main hydrogen bond interactions of both complexes.

Complex form	**Interaction**	**ρ_b**	**$\nabla^2\rho_b$**
Neutral	O47···HB1···O160	0.0169	0.0658
	O55···HB3···O150	0.0155	0.0584
	O62···HB2···O148	0.0122	0.0490

Deprotonated	O53···HB2···O157	0.0337	0.1220
	O54···HB1···O157	0.0259	0.0926
	O63···HB3···O158	0.0235	0.0889

According to the values of ρ_b and $\nabla^2\rho_b$ displayed in Table 2, there is a trend towards larger values for the deprotonated complex and lower values for the neutral complex. This gives a further evidence for the characterization of these hydrogen bonds, which are considered moderately strong for the deprotonated complex and moderately weak for the neutral one. These results were in line with those obtained using NBO method.

The molecular graph of the deprotonated/neutral complex displayed in Figure 10, visualizes clearly the formation of these H-bonds, with the red points (HBn) over the bond path of the H-bond interaction.

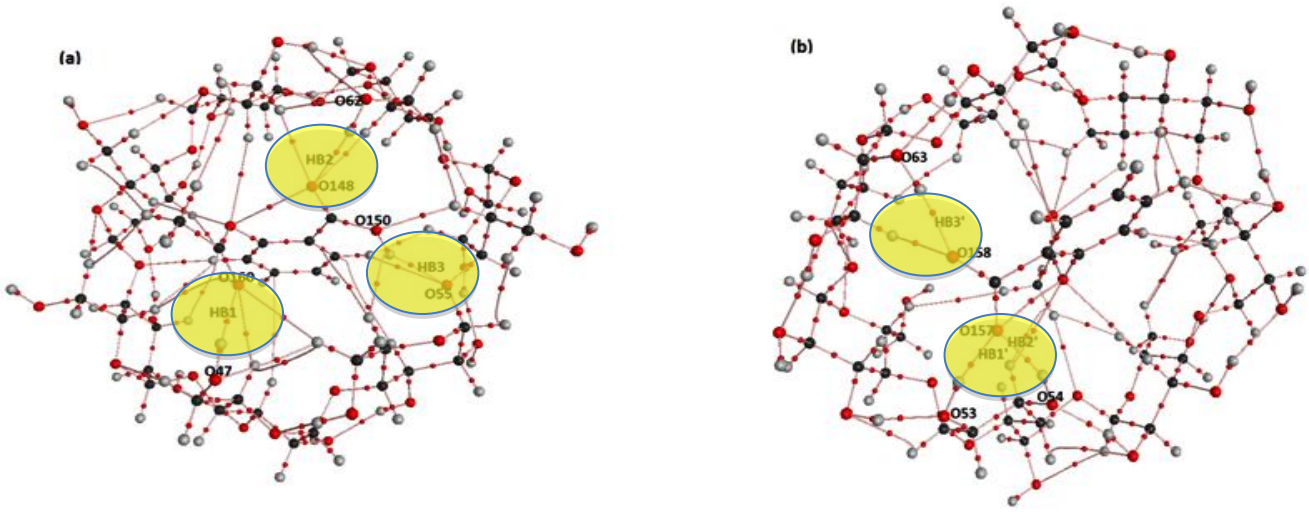

Figure 10. Molecular graph of the main hydrogen bond interactions (the yellow circles shows the most important) of (a) the neutral complex (b) the deprotonated complexes.

3.2.4 The hydrophobic/hydrophilic interactions

The hydrophobic/hydrophilic interaction is discussed based on the interaction between the different moieties of the system. Thus, for the neutral complex, the phenyl group molecule, considered as hydrophobic, is located inside the hydrophobic cavity of the β–CD. However, both

of acetyl and carboxylic groups of aspirin, considered as hydrophilic, are localized on the hydrophilic periphery of the β–CD, in contact with the water molecules. So, the hydrophilic/hydrophobic interactions are favorable to the formation of the neutral complex.

However, for the deprotonated complex, the acetyl hydrophilic group is localized inside the hydrophobic cavity of the β–CD, and the hydrophobic phenyl group is localized outside the cavity in the aqueous medium. So the hydrophobic/hydrophilic interactions are unfavorable to the formation of the deprotonated complex.

3.2.5 Infrared analysis

As the carbonyl groups of aspirin are involved in several hydrogen bonds with β–CD, it seems interesting to study the inclusion effect on these vibration frequencies. For this purpose, the spectra of the complexes and aspirin under both forms are calculated at B3LYP/cc-pvdz level with CH_3CN as a solvent. We will focus only on the CO vibration region of the IR spectra of aspirin (neutral/deprotonated) and their inclusion complexes. The spectrum of the β–CD itself is not is not considered due to the absence of the carbonyl stretching bands (νC=O).

3.2.5.2 Neutral complex

The IR spectrum of aspirin shows a band at 1802 cm^{-1} corresponding to the carbonyl stretching band (νC=O) of the carboxylic group (Figure 11 (a) , Free ASA). This band is shifted towards lower frequency (1744 cm^{-1}) in the inclusion complex ($\Delta\nu$ = 58 cm^{-1}) (Figure 11 (a) , ASA**:** β–CD). Similarly, the carbonyl stretching band (νC=O) of the acetyl group of aspirin located at 1820 cm^{-1}, is shifted to 1773 cm^{-1} in the inclusion complex ($\Delta\nu$ = 47 cm^{-1}). As it is the case for ASA-, the differences in the observed shifts of the carbonyl stretching band (νC=O) can also be explained by the involvement of these two carbonyl groups in the hydrogen bonds with the hydroxyls of β–CD.

In other words, the differences in the observed shifts of the carbonyl stretching band (ν C=O) in the IR spectroscopy constitute the evidence of the formation of the inclusion complex of both forms. Accordingly, IR method can be considered as a suitable technique for the detection of the formation of the inclusion complexes.

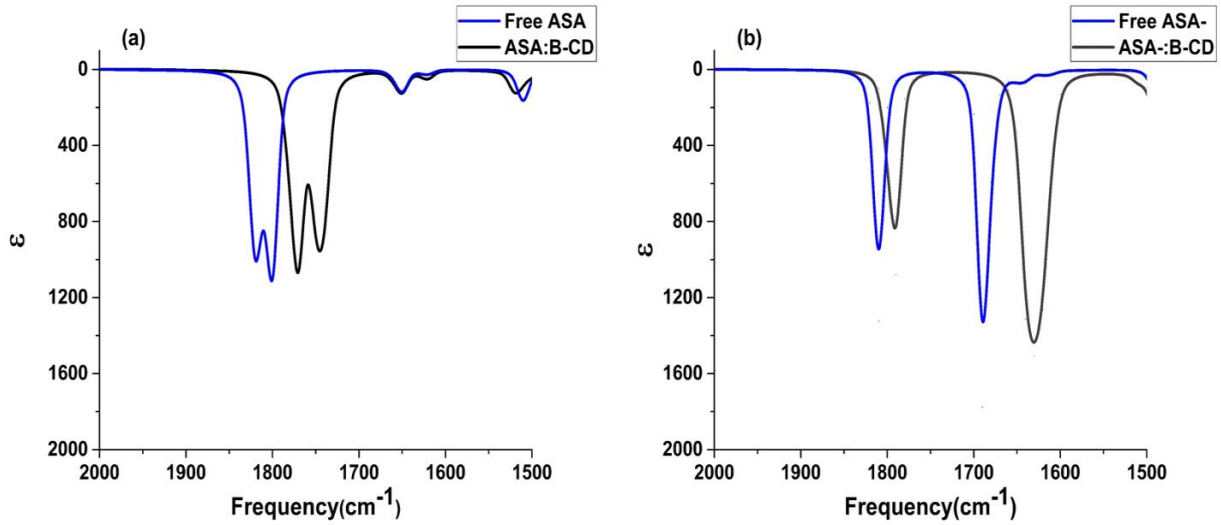

Figure 11. (a) On the left, the computed IR spectra shows the shift of the stretching band of CO in the free aspirin and in the ASA**:**β–CD complex. (b) On the right, the computed IR spectra shows the shift of the stretching band of CO in the free deprotonated aspirin and in the ASA^-**:**β–CD complex

3.2.5.1 Deprotonated complex

The spectra are displayed in Figure 11. Two carbonyl stretching bands (νC=O) frequencies are observed in the IR spectrum of deprotonated aspirin, one located at 1687 cm^{-1} attributed to the two carbonyls of the carboxylate group and the second is located at 1809 cm^{-1} attributed to the carbonyl of the acetyl group (Figure 11 (b), free ASA^-). The carbonyl stretching band (νC=O) of the carboxylate group is considerably shifted to the lower frequencies, located at 1634 cm^{-1} ($\Delta\nu$ = 53cm^{-1}) (Figure 11 (b), ASA^-**:**β–CD).

This difference is more significant in the CO groups of carboxylate because they are involved in three hydrogen bonds, which is not the case of the CO group of acetyl not involved in any H-bonds.

3.2.6 UV analysis

We calculated the ultraviolet-visible spectra of both forms of free aspirin, free β–CD and their complexes in order to get more quantitative information data on these complexes.

TD-DFT calculations were made on neutral and deprotonated aspirin, the β–CD and their inclusion complex at the B3LYP/ cc-pvdz level in ethanol. The obtained spectra are shown in Figure 12.

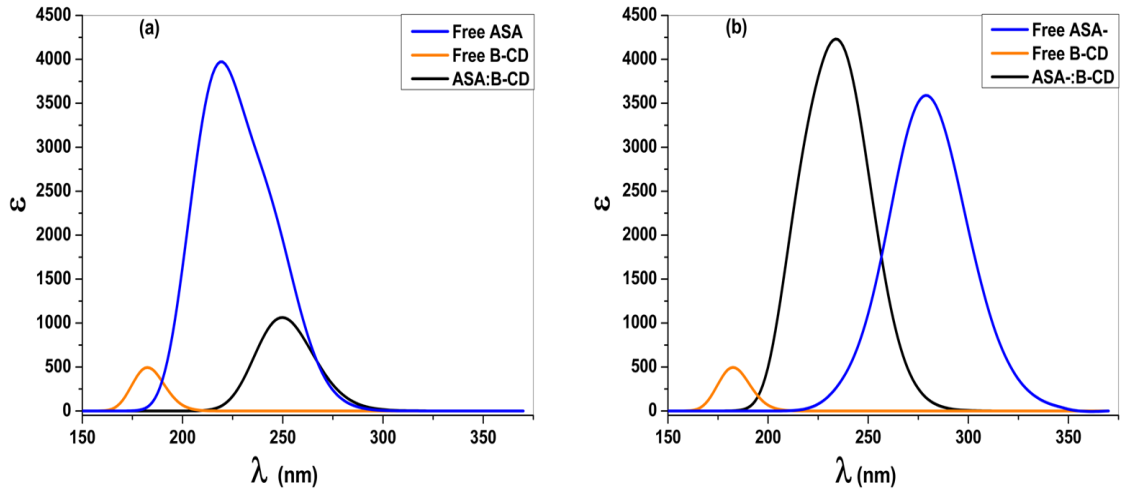

Figure 12 (a) On the left, computed UV spectra of free neutral aspirin, β–CD and the ASA**:** β–CD complex. (b) On the right, computed UV spectra the deprotonated aspirin, β–CD and the ASA^-**:** β–CD complex.

3.2.6.1 Neutral complex

The computed UV spectrum of the inclusion complex shows a band with a maximum absorption located at 251 nm (Figure 12 (a)). Since there is no absorption band from β–CD and the maximum absorbance of aspirin is located at 220 nm this leads to consider the existence of a new component other than aspirin and β–CD. If this band is specific to the formed complex, it should be made up of transitions between aspirin and cyclodextrin. This is only be possible if the energy differences between the frontier orbitals of aspirin and β–CD are reduced.

The transitions and their obtained wavelengths from the UV spectrum of the complex are shown in Table 3. The transitions involve six occupied orbitals (343-348) considered here as nearly degenerated HOMO. They target to the same unoccupied orbital 349. We considered it as a unique LUMO.

Table 3. The different transitions with their wavelengths observed in the computed UV spectrum of the ASA**:**β–CD complex.

N° of the transition	HOMO-LUMO	Wavelength (nm)
1	348-349	262
2	347-349	259
3	346-349	256
4	345-349	253
5	344-349	251
6	343-349	249

The HUMOs and LUMOs of the neutral complex are shown in Figure 13.

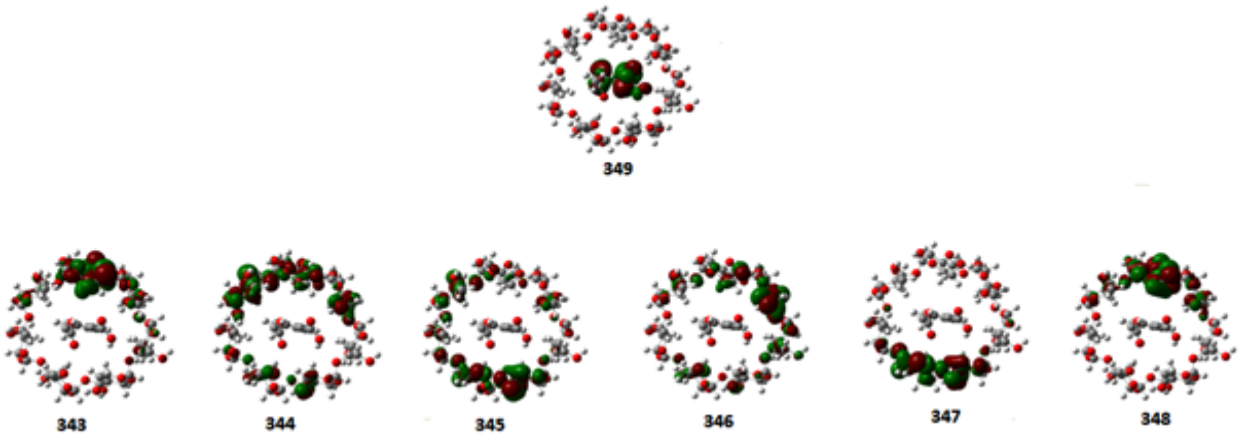

Figure 13. The different orbitals HOMO and LUMO of the ASA:β–CD complex (neutral).

We display in Figure 13, the LUMO (349) and the six aformentioned HOMO (343-348). The LUMO is located on the aspirin and the six HOMOs spread over the β–CD. Thus, the six HOMO-LUMO transitions correspond to a donation from the β–CD towards aspirin. This can be explained by the richness of the electronic density in cavity generated by the oxygen atoms of β–CD that will affect the electronic energy state of aspirin, which becomes close to those of β–CD.

3.2.6.2 Deprotonated complex

The UV-visible computed spectrum of deprotonated aspirin (Figure 12 (b)) shows a band located at 280 nm. The absorption maximum of the spectrum of the inclusion complex is shifted to 232 nm, which is also an evidence of the formation of a new component.

The transitions and their obtained energies from the UV-visible spectrum of the complex are shown in Table 4. The transitions involve three occupied orbitals (346-348) that we name as

nearly degenerated HOMOs. They target to three unoccupied orbital (349-351), that we name as as nearly degenerated LUMOs.

Table 4: The different transitions with their wavelengths observed in the UV spectrum of the ASA^- **:**β–CD complex.

N° of the transition	**HOMO-LUMO**	**Wavelength λ (nm)**
1	348-349	244
2	348-350	241
3	347-349	232
4	347-350	226
5	348-351	216
6	346-349	213

The HUMOs and LUMOs of the deprotonated complex as computed in the ground state are shown in Figure 14. As it can be seen, three LUMO orbitals are spread over aspirin (349, 350 and 351). Whereas, for the HOMO orbitals, two orbitals (346 and 347) spread over the β–CD and one (348) is over aspirin. Thus, the transitions from the HOMO (346 and 347) characterize the inclusion complex because these are the transitions from β–CD towards aspirin. However, those from the HOMO (348) are related to the internal electronic transitions in aspirin itself. This can be explained by the effect of the partial inclusion. Indeed, an important part of aspirin remains outside of the cavity, retaining a part of its intrinsic properties. On the contrary, in the neutral complex, aspirin is completely embedded inside the cavity, and it loses entirely its intrinsic properties.

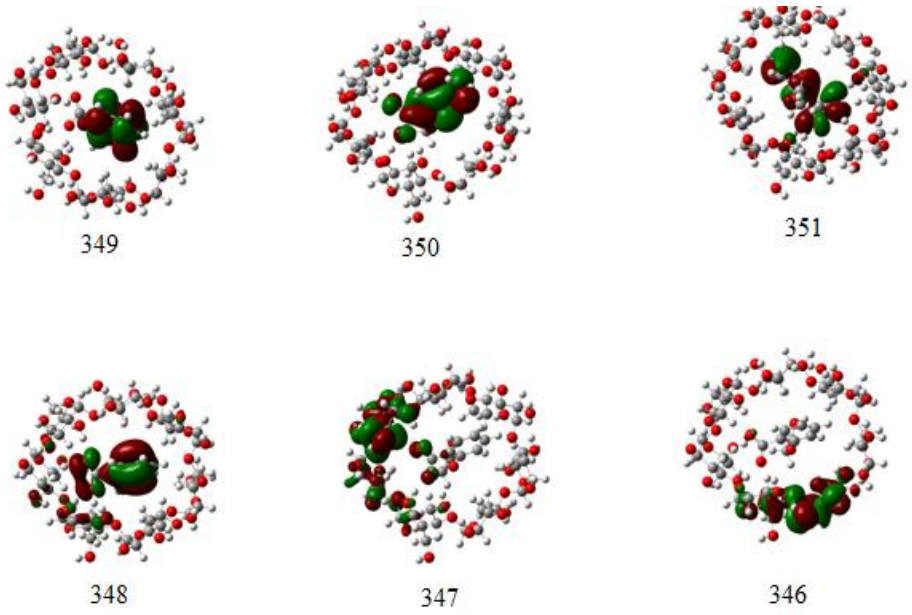

Figure 14. The different orbitals HOMO and LUMO of the ASA^-**:** β–CD complex.

Conclusions

Molecular dynamics and quantum mechanics applied to study the complexation process of aspirin and deprotonated aspirin with β–CD give the neutral aspirin: β–CD complex more favorable than the deprotonated one. In the neutral complex, the penetration occurs through the two entrances, and the more favorable orientation is that wherein the acetyl group penetrates first (orientation A). Moreover, the complexation process can be considered as irreversible. However, in the deprotonated complex, the penetration occurs through both of the wide and the narrow rims, and the complexation process is to be considered as reversible. The lowest energy minimum structures obtained by quantum mechanics show a deep inclusion in aspirin:β–CD complex and partial in the deprotonated complex. The degree of penetration (deep or partial) is characterized by UV spectroscopy by determining the origin of the different electronic transitions.

The NBO method describes a weak H-bond interactions in the neutral complex, and moderately strong in the deprotonated one; the AIM method confirms this and it also visualizes clearly the formation of these H-bonds as well. The hydrophobic/hydrophilic interactions are favorable for the neutral complex and unfavorable for the deprotonated one.

The shifts of the CO vibration of aspirin observed in calculated IR spectroscopy show the effect of the inclusion of aspirin inside the cavity and also they constitute the evidence of the formation of the inclusion complex in both cases.

Acknowledgements

The investigation was supported by the Algerian Ministry of higher education and scientific research and the research center in industrial technology, Algiers (Algeria). Aix-Marseille University is gratefully acknowledged for an invited professor position (DK) + MESOCENTRE.

ASSOCIATED CONTENT

The input files of aspirin and β–CD.

(supporting_file.pdf).

AUTHOR INFORMATION

Corresponding Author

*(K.D.) E-mail (khatmi.djameleddine@gmail.com). Tel : (33) 751339640

Present address

Department of chemistry, University of Guelma, 24000, Algeria

Co-authors

Belgacem Bezzina (bezzinabelgacem@yahoo.fr)

Rayenne Djémil (messdjem@gmail.com)

Yannick Carissan (yannick.carissan@univ-amu.fr)

Pr Stéphane Humbel (stephane.humbel@univ-amu.fr)

Fatiha Madi (fatiha_madi@yahoo.fr)

Leila Nouar (leilanoua@yahoo.fr)

Author Contributions

The manuscript was written through contributions of all authors. All authors have given approval to the final version of the manuscript. ‡These authors contributed equally.

Notes

The authors declare no competing financial interest.

Funding Sources

The investigation was supported by the Algerian Ministry of higher education and scientific research and the research center in industrial technology, Algiers (Algeria). DJ acknowledges Aix-Marseille University (France) for an invited professor position.

REFERENCES

1. Szente L, Szejtli J (2004) Cyclodextrins as food ingredients, Trends in Food Science & Technology 15(3):137-142.
2. Szente L, Szemán J, (2013) Cyclodextrins in analytical chemistry, Host–guest type molecular recognition. *Analytical chemistry 85*(17):8024-8030.
3. Lehn JM, (1988) Supramolecular chemistry - scope and perspectives: molecules - supermolecules – molecular devices. J Inclusion Phenom 6 (4):351–396.
4. Szente L, Szejtli J, (1999) Highly soluble cyclodextrin derivatives: chemistry, properties, and trends in development. Adv Drug Deliver Rev 36 (1):17–28.
5. Marques HMC, (2010) A review on cyclodextrin encapsulation of essential oils and volatiles. Flav Frag J 25 (5):313–326.
6. Landy D, Tetart F, Truant E, Blach P, Fourmentin S, Surpateanu G, (2007) Development of a competitive continuous variation plot for the determination of inclusion compounds stoichiometry. J Incl Phenom Macro 57 (1-4):409–413.
7. Komiyama M, Bender ML, (1978) Thermodynamic studies of the cyclodextrin-accelerated cleavage of phenyl esters. J Am Chem Soc 100 (14):4576–4579.
8. Szejtli J, Bolla PE, Kajtar M (1982) The ß-cyclodextrin inclusion complex of menadione (vitamin K3). Pharmazie 37 (10):725–728.

9. Varady J, Wu X, Wang S, (2002) Competitive and reversible binding of a guest molecule to its host in aqueous solution through molecular dynamics simulation, Benzyl alcohol/β-cyclodextrin system. The Journal of Physical Chemistry B 106 (18):4863-4872.

10. Challa R, Ahuja A, Ali J, Khar RK, (2005**)** Cyclodextrins in drug delivery, an updated review. AAPS PharmSciTech 6 (2):E329–E357.

11. Loftsson T, Duchene D, (2007) Cyclodextrins and their pharmaceutical applications. Int J Pharm 329 (1-2):1–11.

12. Kanaka DDN, Prameela RA, Muneer AM, SaiKumar K, Kaushik JS, (2010) Cyclodextrins in pharmacy - an overview. Journal of Global Pharma Technology 2 (11):1–10.

13. Salustio PJ, Pontes P, Conduto C, Sanches I, Carvalho C, Arrais J, Marques, HMC, (2011) Advanced technologies for oral controlled release, cyclodextrins for oral controlled release. AAPS Pharm Sci Tech 12 (4):1276–1292.

14. Yin JJ, Zhou ZW, Zhou SF, (2013) Cyclodextrin-based targeting strategies for tumor treatment. Drug Deliv Transl Res 3 (4):364–374.

15. Crini G, (2014) Review: a history of cyclodextrins. Chem Rev 114 (21):10940–10975.

16. Duchene D, Ponchel G, Bochot A, (2005) New uses of cyclodextrins. Eur J Pharm Sci 25: S1–S2.

17. Duchene D, Bochot A, Loftsson T, (2009) Cyclodextrins and their use in pharmacy and cosmetology. S.T.P. Pharma Pratiques 19 (1):15–27.

18. Moore N, Ganse E V, Parc JML, Wall R, Schneid H, Farhan M, Verrière F, Pelen F, (1999) The PAIN Study: Paracetamol, Aspirin and Ibuprofen New Tolerability Study. Clin Drug Investig 18 (2): 89–98.

19. Impicciatore P, Pandolfini C, Casella N, Bonati M (1997) Reliability of Health Information for the Public on the World Wide Web: Systematic Survey of Advice on Managing Fever in Children at Home. BMJ 314 (7098):1875.

20. Chaudhary R, Bliden KP, Garg J, Mohammed N, Tantry U, Mathew D, Toth PP, Franzese C, Gesheff M, Pandya S, et al (2016) Statin Therapy and Inflammation in Patients with Diabetes Treated with High Dose Aspirin. J Diabetes Complications 30 (7):1365–1370.

21. Amory JK, Amory DW, (2007) Dosing Frequency of Aspirin and Prevention of Heart Attacks and Strokes. Am J Med 120 (4):e5.

22. Viola F, Lin-Schmidt X, Bhamidipati C, Haverstick DM, Walker WF, Ailawadi G, Lawrence MB, (2016) Sonorheometry Assessment of Platelet Function in Cardiopulmonary Bypass Patients: Correlation of Blood Clot Stiffness with Platelet Integrin αIIbβ3 Activity, Aspirin Usage, and Transfusion Risk. Thromb Res 138:96–102.

23. Rothwell PM, Wilson M, Elwin CE, Norrving B, Algra A, Warlow CP, Meade TW, (2010) Long-Term Effect of Aspirin on Colorectal Cancer Incidence and Mortality, 20-Year Follow-up of Five Randomised Trials. The Lancet 376 (9754):1741–1750.

24. Jiang MJ, Dai JJ, Gu DN, Huang Q, Tian L, (2016) Aspirin in Pancreatic Cancer, Chemopreventive Effects and Therapeutic Potentials. Biochim Biophys Acta 1866 (2):163–176.

25. Rainsford KD, (1984) Aspirin and the Salicylates; Butterworths.

26. Rainsford KD, (2004) Aspirin and Related Drugs, Ed CRC Press.

27. Castronuovo G, Niccoli M, (2013) Thermodynamics of Inclusion Complexes of Natural and Modified Cyclodextrins with Acetylsalicylic Acid and Ibuprofen in Aqueous Solution at 298 K. Thermochim Acta 557:44–49.

28. Penner MJ, (1989) Aspirin Abolishes Tinnitus Caused by Spontaneous Otoacoustic Emissions, A Case Study, Arch Otolaryngol Head Neck Surg 115 (7):871–875.

29. Tee OS, Takasaki BK, (1985) The Cleavage of Aspirin by α-and β-Cyclodextrins in Basic Aqueous Solution. Can J Chem 63 (12):3540–3544.

30. Carstensen J.T , Attarchi F , Hou X-P (1985). Decomposition of aspirin in the solid state in the presence of limited amounts of moisture. J. Pharm. Sci 74(7):741-745.

31. Tegge G, Szejtli J, (1982) Cyclodextrins and Their Inclusion Complexes (Cyclodextrine Und Ihre Einschlußkomplexe). Verlag Der Ungarischen Akademie Der Wissenschaften. Akadémiai Kiadó, Budapest 34 (11):395–395.

32. Dodziuk H, (2006) Front Matter, In Cyclodextrins and Their Complexes; Ed.; Wiley-VCH Verlag GmbH & Co. KGaA pp I–XVII.

33. Cheng J, Wang Z, (2012) Synthesis of 5-Fluorouracil Acetic Acid Prodrugs of #x0DF;-Cyclodextrin at the Secondary Hydroxyl Side as Potential Colon-Specific Delivery Systems. In 2012 International Conference on Biomedical Engineering and Biotechnology :565–566.

34. Loftsson T Ólafsdóttir BJ, Friðriksdóttir H, Jónsdóttir S, (1993) Cyclodextrin Complexation of NSAIDSs: Physicochemical Characteristics. Eur J Pharm Sci 1 (2):95–101.

35. Kalathil AA, Kumar A, Banik B, Ruiter TA, Pathak RK, Dhar S, (2015) New Formulation of Old Aspirin for Better Delivery. Chem Commun 52 (1):140–143.

36. Shende PK, Trotta F, Gaud RS, Deshmukh K, Cavalli R, Biasizzo M, (2012) Influence of Different Techniques on Formulation and Comparative Characterization of Inclusion Complexes of ASA with β-Cyclodextrin and Inclusion Complexes of ASA with PMDA Cross-Linked β-Cyclodextrin Nanosponges. J Incl Phenom Macrocycl Chem 74 (1–4): 447–454.

37. Miranda JCD; Martins TEA, Veiga F, Ferraz HG, (2011) Cyclodextrins and Ternary Complexes: Technology to Improve Solubility of Poorly Soluble Drugs. Braz J Pharm Sci 47 (4):665–681.

38. Malenkovskaya MA, Grachev MK, Levina II, Nifant'ev EE, (2013) Amphiphilic Conjugates of β-Cyclodextrin with Acetylsalicylic and 2-(4-Isobutylphenyl)propionic Acids Russ J Org Chem 49 (12):1777–1782.

39. Nishioka F, Nakanishi I, Fujiwara T, Tomita K, (1984) The Crystal and Molecular Structure of the β-Cyclodextrin Inclusion Complex with Aspirin and Salicylic Acid. J Incl Phenom 2 (3–4):701–714.

40. Loftsson T, Brewster ME, (1996) Pharmaceutical Applications of Cyclodextrins. Drug Solubilization and Stabilization. J Pharm. Sci 85 (10):1017–1025.

41. Rajagopalan P, Penial P, (2013) Study of the spectral properties of inclusion complex of aspirin with hydroxy propyl β - cyclodextrin. Int J Pharm Clin Sci Int 3 (4):24–28.

42. Nakai Y, Nakajima S-I, Yamamoto K, Terada K, Konno T,(1978) Effects of grinding on physical and chemical properties of crystalline medicinals with microcrystalline cellulose. III. Infrared spectra of medicinals in ground mixtures. Chemical and Pharmaceutical Bulletin 26(11): 3419-3425.

43. Iohara D, Yoshida K, Yamaguchi K, Anraku M, Motoyama K, Arima H, Uekama K, Hirayama F, (2012) Cyclodextrin-Induced Change in Crystal Habit of Acetylsalicylic Acid in Aqueous Solution. Cryst Growth Des 12 (4):1985–1991.

44. Nakai Y, Fukuoka E, Nakajima S, Yamamoto K, (1977) Effects of Grinding on Physical and Chemical Properties of Crystalline Medicinals with Microcrystalline Cellulose. I. Some Physical Properties of Crystalline Medicinals in Ground Mixtures. Chem Pharm Bull (Tokyo) 25 (12):3340–3346.

45. Nakai Y, Yamamoto K, Terada K, Ueno Y, (1986) Effects of the Degree of Polymerization of Oligosaccharides on the Properties of Ground Mixtures. Chem Pharm Bull (Tokyo) 34 (1):315–319.

46. Kitchin SJ, Halstead TK, (1999) Solid-state2H NMR Studies of Methyl Group Dynamics in Aspirin and Aspirin · β-Cyclodextrin. Appl Magn Reson 17 (2–3):283–300.

47. Choi HS, (1991) Structure Study of Inclusion Complex of ß Cyclodextrine and Aspirin. J. Pharm Investig 21 (4):223–230.

48. Nakai Y, Yamamoto K, Terada K, Akimoto K, (1984) The Dispersed States of Medicinal Molecules in Ground Mixtures with α- or β-Cyclodextrin. Chem Pharm Bull (Tokyo) 32 (2):685–691.

49. Fukahori T, Kondo M, Nishikawa S, (2006) Dynamic Study of Interaction between Beta-Cyclodextrin and Aspirin by the Ultrasonic Relaxation Method. J Phys Chem B 110 (9):4487–4491.

50. Sancho MI, Andujar S, Porasso RD, Enriz RD, (2016) Theoretical and Experimental Study of Inclusion Complexes of β-Cyclodextrins with Chalcone and 2′,4′-Dihydroxychalcone. J Phys Chem B 120 (12):3000–3011.

51. Chen S, Han Z, Zhang D, Zhan J, (2014) Theoretical Study of the Inclusion Complexation of TCDD with Cucurbit[n]urils. RSC Advances 4 (94):52415–52422.

52. Punkvang A, Saparpakorn P, Hannongbua S, Wolschann P, Beyer A, Pungpo P, (2010) Investigating the Structural Basis of Arylamides to Improve Potency against M. Tuberculosis Strain through Molecular Dynamics Simulations. Eur J Med Chem 45 (12):5585–5593.

53. Pan W, Zhang D, Zhan J, (2011) Theoretical Investigation on the Inclusion of TCDD with β-Cyclodextrin by Performing QM Calculations and MD Simulations. J Hazard Mater 192 (3):1780–1786.

54. Zhang H, Feng W, Li C, Tan T, (2010) Investigation of the Inclusions of Puerarin and Daidzin with β-Cyclodextrin by Molecular Dynamics Simulation. J Phys Chem B 114 (14): 4876–4883.

55. Madi F, Khatmi D, Dhaoui N, Bouzitouna A, Abdaoui M, Boucekkine A, (2009) Molecular Model of CENS Piperidine Beta-CD Inclusion Complex: DFT Study. Comptes Rendus Chim 12 (12):1305–1312.

56. Yahia OA, Khatmi DE, (2009) Theoretical Study of the Inclusion Processes of Venlafaxine with Beta-Cyclodextrin. J Mol Struct 912 (1–3):38–43.

57. Madi F, Khatmi DE, Largate L, (2010) Theoretical Approach in the Study of the Inclusion Processes of Sulconazole with Beta-Cyclodextrin. J Mol Liq 154 (1):1–5.

58. Kerwin SM, (2010) ChemBioOffice Ultra 2010 Suite. J Am Chem Soc 132 (7):2466–2467.

59. Bolton EE, Wang Y, Thiessen PA, Bryant SH, (2008) Integrated Platform of Small Molecules and Biological Activities. In Annual Reports in Computational Chemistry; Spellmeyer, R. A. W. and D. C., Ed.; Elsevier (4):217–241.

60. Malde AK, Zuo L, Breeze M, Stroet M, Poger D, Nair PC, Oostenbrink C, Mark AE, (2011) An Automated Force Field Topology Builder (ATB) and Repository: Version 1.0. J. Chem Theory Comput 7 (12):4026–4037.

61. Schmid N, Eichenberger AP, Choutko A, Riniker S, Winger M, Mark AE, Gunsteren WFV (2011) Definition and Testing of the GROMOS Force-Field Versions 54A7 and 54B7. Eur Biophys J 40 (7):843-856.

62. Abraham MJ, Murtola T, Schul R, Páll S, Smith JC, Hess B, Lindahl E, (2015) GROMACS: High Performance Molecular Simulations through Multi-Level Parallelism from Laptops to Supercomputers. Software, 1–2:19–25.

63. Van Der Spoel D, Lindahl E, Hess B, Groenhof G, Mark AE, Berendsen HJC, (2005) GROMACS: Fast, Flexible, and Free. J Comput Chem 26 (16):1701–1718.

64. Frisch M, Trucks G, Schlegel H, Scuseria G, Robb M, Cheeseman J, Scalmani G, Barone V, Mennucci B, Petersson G, et al (2013) Gaussian 09, Revision D.01. Gaussian 09 Revis. B01 Gaussian Inc Wallingford CT.

65. Becke AD, (1993) Density-functional Thermochemistry. III. The Role of Exact Exchange. J Chem Phys 98 (7):5648–5652.

66. Lee C, Yang W, Parr RG, (1988) Development of the Colle-Salvetti Correlation-Energy Formula into a Functional of the Electron Density. Phys Rev B 37 (2):785–789.

67. Vosko SH, Wilk L, Nusair M, (1980) Accurate Spin-Dependent Electron Liquid Correlation Energies for Local Spin Density Calculations: A Critical Analysis. Can J Phys 58 (8):1200–1211.

68. Stephens PJ, Devlin FJ, Chabalowski CF, Frisch MJ, (1994) Ab Initio Calculation of Vibrational Absorption and Circular Dichroism Spectra Using Density Functional Force Fields. J Phys Chem 98 (45):11623–11627.

69. Dunning JTH, (1989) Gaussian Basis Sets for Use in Correlated Molecular Calculations. I. The Atoms Boron through Neon and Hydrogen. J Chem Phys 90 (2):1007–1023.

70. Reed AE, Weinhold F, (1985) Natural Localized Molecular Orbitals. J Chem Phys 83 (4): 1736–1740.

71. *Hydrogen Bonding—New Insights*; Grabowski, S. J., Ed.; Springer Netherlands, 2006.

72. Jeffrey, G. A. *An Introduction to Hydrogen Bonding*, 1 edition.; Oxford University Press: New York, 1997.

73. Perrin, C. L.; Nielson, and J. B. "Strong" Hydrogen Bonds in Chemistry and Biology. *Annu. Rev. Phys. Chem.* **1997**, *48* (1), 511–544.

74. Humbel, S. Short Strong Hydrogen Bonds: A Valence Bond Analysis. *J. Phys. Chem. A* **2002**, *106* (22), 5517–5520.

75. Biegler-König F, Schönbohm J (2002) Update of the AIM2000-Program for Atoms in Molecules. J Comput Chem 23 (15):1489–1494.

76. Gross EKU, Kohn W, (1990) Time-Dependent Density-Functional Theory. In Advances in Quantum Chemistry; Löwdin, P.-O., Ed.; Density Functional Theory of Many-Fermion Systems; Academic Press (21):255–291.

77. Cortesguzman F, Bader R, (2005) Complementarity of QTAIM and MO Theory in the Study of Bonding in Donor-acceptor Complexes. Coord Chem Rev 249 (5–6):633–662.

78. Grabowski SJ, (2006) Hydrogen Bonding—New Insights, Ed.; Springer Netherlands.

79. Jeffrey GA, (1997) An Introduction to Hydrogen Bonding, 1 edition, Oxford University Press: New York.

80. Perrin CL, Nielson JB, (1997) "strong" Hydrogen Bonds in Chemistry and Biology. Annu Rev Phys Chem 48 (1):511–544.

81. Humbel S, (2002) Short Strong Hydrogen Bonds: A Valence Bond Analysis. J Phys Chem 106 (22):5517–5520.

82. Attoui-Yahia O, Khatmi D, Kraim K, Ferkous F, (2015) Hydrogen Bonding Investigation in Pyridoxine/Beta-Cyclodextrin Complex Based on QTAIM and NBO Approaches. J Taiwan Inst Chem Eng 47:91–98.

83. Djemil R, Attoui-Yahia O, Khatmi D, (2015) DFT-ONIOM Study of the Dopamine-Beta-CD Complex: NBO and AIM Analysis. Can J Chem 93 (10):1115–1121.